



Structural dependence of corrosion resistance of amorphous carbon films against nitric acid[☆]



Atsuyuki Takarada^a, Tsuneo Suzuki^b, Kazuhiro Kanda^c, Masahito Niibe^c, Masayuki Nakano^d, Naoto Ohtake^a, Hiroki Akasaka^{a,*}

^a Department of Mechanical Sciences and Engineering, Tokyo Institute of Technology, 2-12-1 Ookayama, Meguro-ku, Tokyo 152-8552, Japan

^b Extreme Energy-Density Research Institute, Nagaoka University of Technology, 1603-1 Kamitomioka, Nagaoka, Niigata 940-2188, Japan

^c Laboratory of Advanced Science and Technology for Industry, University of Hyogo, 3-1-2 Koto, Kamigori-cho, Ako-gun, Hyogo 678-1205, Japan

^d Department of Chemical Science and Engineering, Tokyo National College of Technology, 1220-2 Kunugida, Hachioji, Tokyo 193-0997, Japan

ARTICLE INFO

Article history:

Received 27 September 2014

Received in revised form 8 November 2014

Accepted 10 November 2014

Available online 21 November 2014

Keywords:

Amorphous carbon
Structural dependence
Corrosion resistance
Nitric acid

ABSTRACT

To investigate the structural dependence of the corrosion resistance of amorphous carbon (*a*-C:H) films, three different types of *a*-C:H films etched by nitric acid were evaluated using a surface plasmon resonance (SPR) device with a multilayer structure consisting of an *a*-C:H layer on Ag. Two non-hydrogenated amorphous carbon (*a*-C) films and one hydrogenated *a*-C:H film were synthesized to estimate the effects of the sp^2/sp^3 ratio and hydrogenation, respectively. A flow cell for the introduction of nitric acid solution was placed on the amorphous carbon layer of the multilayer structure. A 0.3 mM nitric acid solution was used in the etching tests. The Kretschmann configuration was used for SPR measurement, and the SPR angle was determined as the angle with minimum reflectivity. The SPR angle decreased with increasing duration of nitric acid injection into the flow cell, indicating that the film was corroded by the nitric acid. The thickness of the films was calculated from the SPR angle. The rates of decrease in the thickness were 2.2, 0.8, and 1.6 nm/h for the *a*-C films with lower and higher sp^2 contents and the 17 at.% hydrogenated *a*-C:H film, respectively. Although the hydrogen content had little effect on the rate of change in the film thickness, the film thickness clearly decreased with decreasing sp^2/sp^3 ratio. These results indicate that the sp^2/sp^3 ratio is an important factor determining the chemical resistance to nitric acid solution.

© 2014 Elsevier B.V. All rights reserved.

1. Introduction

Hydrogenated amorphous carbon (*a*-C:H) films have been applied to mechanical parts owing to their high hardness and low friction coefficient [1–3]. It is well known that these mechanical properties depend on the structure of the *a*-C:H films. These films consist of carbon and hydrogen atoms, where the carbon atoms mainly form sp^2 - and sp^3 -hybridized bonds. Robertson proposed a tertiary diagram consisting of the sp^2 , sp^3 , and hydrogen contents to promote understanding of the *a*-C:H film structure [4–6]. Relationships between the mechanical properties and the structure of *a*-C:H films have often been discussed using this tertiary diagram. The mechanical properties of *a*-C:H films have been reported in many papers, and the relationship between the properties and film structure is now well understood [6,7].

On the other hand, some reports have indicated that *a*-C:H films have high chemical resistance [8,9], and it has been shown that *a*-C:H

films can potentially be used as coatings for microfluidic devices [9]. In studies on the chemical resistance of such films, samples coated with an *a*-C:H film are usually dipped in a chemical solution, and cross sections of the dipped samples are observed using a scanning electron microscope. In these studies, the process used to evaluate the etching requires a long time and cannot be used to estimate the decrease in film thickness. Hence, the relationship between the chemical resistance of *a*-C:H films and the film structure has not been clarified. A quantitative method for evaluating the chemical resistance of *a*-C:H films in a short time is required. Sasaki et al. reported the etching rate of an *a*-C:H film by nitric acid solution using the phenomenon of surface plasmon resonance (SPR) [10]. The chemical resistance of an *a*-C:H film can be quantitatively estimated using their method. In this paper we report the structural dependence of the corrosion resistance of *a*-C:H films using this method.

SPR is the resonance between an evanescent wave on a metal surface and a surface plasmon wave [11–16], as shown in Fig. 1. At a thin metal film on a glass prism, light from a laser is irradiated from the glass, an evanescent wave penetrates through the metal film, and plasmon waves are also excited on the opposite side of the thin metal film [11–13]. When the wave numbers of the surface plasmon and

[☆] Authorship statement: The submission of the manuscript has been approved by all co-authors.

* Corresponding author.

E-mail address: akasaka@mech.titech.ac.jp (H. Akasaka).

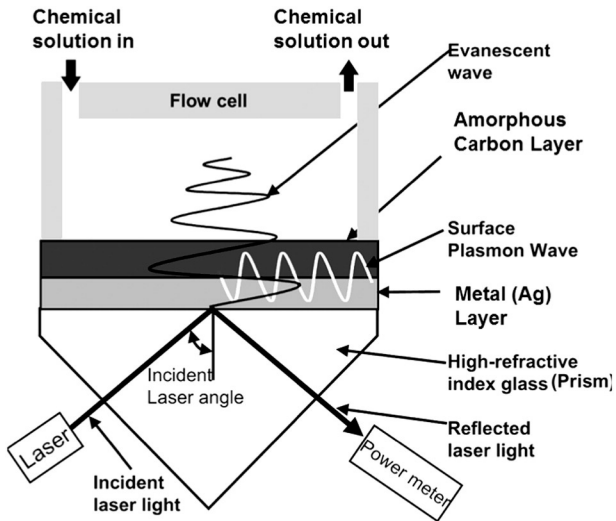


Fig. 1. Schematic illustration of SPR measurement device with the *a*-C:H multilayer structure and the flow cell.

evanescent waves are equal, SPR occurs. The SPR condition depends on the incident angle of the laser light because these waves depend on the incident angle of the laser light [16]. Under the SPR condition, the intensity of the reflected laser light from the back side of the thin metal film markedly decreases. The incident angle of the laser light under this condition is defined as the SPR angle (θ_{SPR}). The intensity of a plasmon wave depends on the refractive index of the metal surface. Hence, the refractive index changes with the configuration on the metal film surface, leading to a shift in θ_{SPR} . The area where this change in the refractive index can be detected is generally less than 200 nm above the metal film; this distance is mainly determined by the penetration distance of the evanescent wave [17]. The detection of a change on a metal surface such as a decrease in the *a*-C:H film thickness due to a chemical reaction is based on the concept of detecting a change in the refractive index. We have already reported the relationship between the film thickness on an Au layer and the shift in θ_{SPR} , and we proved its validity by comparing film thicknesses obtained by X-ray reflectivity and SPR measurements [18]. When a film with a thickness of nanometer order is deposited on a thin metal film, as shown in Fig. 1, a decrease in the film thickness due to a chemical reaction can be detected.

To investigate the structural dependence of the corrosion resistance of *a*-C:H films, three types of *a*-C:H films were deposited on metal surfaces. To clarify the sp^2/sp^3 ratio dependence, two non-hydrogenated amorphous carbon (*a*-C) films were deposited. To determine the effect of hydrogenation, an *a*-C:H film was also deposited on a metal layer. It is well known that graphite can react with nitric acid solution. Since an *a*-C:H film contains graphitic components, we chose nitric acid as the chemical reagent. We attempted to detect the decrease in the thickness of the *a*-C:H film due to the chemical reaction through the detection of SPR on the *a*-C:H/metal multilayer structure shown in Fig. 1. Furthermore, the rate of decrease in the thickness of the films due to the reaction with nitric acid was estimated using an SPR device with a multilayer structure.

2. Experimental method

Fig. 1 shows the multilayer structure used for SPR detection. S-TIH11 optical glass with dimensions of $25 \times 25 \times 1 \text{ mm}^3$ and a refractive index of 1.778 was used as the substrate for the SPR device with the *a*-C:H/metal/glass structure. A silver (Ag) layer was prepared as the metal layer on the S-TIH11 glass by magnetron sputtering in argon gas using an Ag target (99.999%). *a*-C:H and *a*-C films were synthesized on Ag/S-TIH11 glass by two deposition methods. Two types of *a*-C films were synthesized using a filtered cathodic vacuum arc system (FCVA; Nanofilm Technology/Shimadzu DLC-200) with an integrated off-plane double bend (S-bend) [19]. Before deposition, the oxidation layer was removed by argon ion irradiation. The deposition chamber was evacuated to 10^{-4} Pa using a turbo molecular pump. A graphite target (99.999%) was used as the carbon source. Two *a*-C films were individually synthesized at substrate bias voltages of 100 and 400 V. In this paper, the samples deposited at these bias voltages of 100 and 400 V are denoted as "*a*-C 100 V" and "*a*-C 400 V", respectively. One *a*-C:H film was deposited by pulse plasma chemical vapor deposition (CVD) [20]. Before deposition, the oxidation layer was removed by argon ion irradiation. Acetylene gas with a flow rate of $20 \text{ cm}^3/\text{min}$ was used as the carbon source. A pulsed bias voltage of -2.0 kV with a frequency of 14.4 kHz was applied to the substrate. This sample is denoted as "*a*-C:H CVD" in this paper. The deposition duration for each *a*-C and *a*-C:H film layer was controlled so that the film thickness was less than 100 nm, which is the limit of detection in SPR measurement [16]. To observe microstructural change, the amorphous carbon film deposited on a Si(100) substrate was conducted with an immersion test. In this

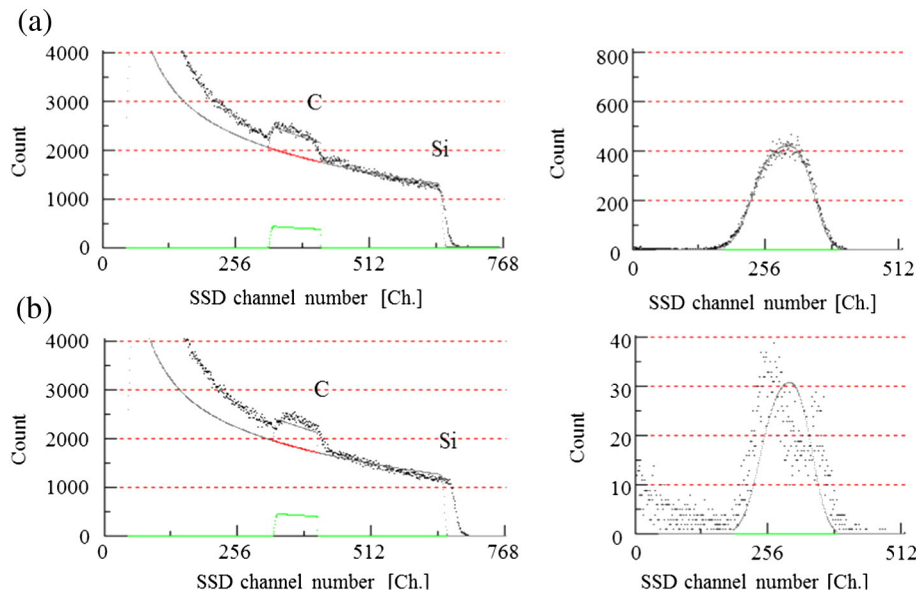


Fig. 2. RBS (left) and ERDA (right) spectra for *a*-C films deposited by FCVA (a) and *a*-C:H films deposited by CVD (b).

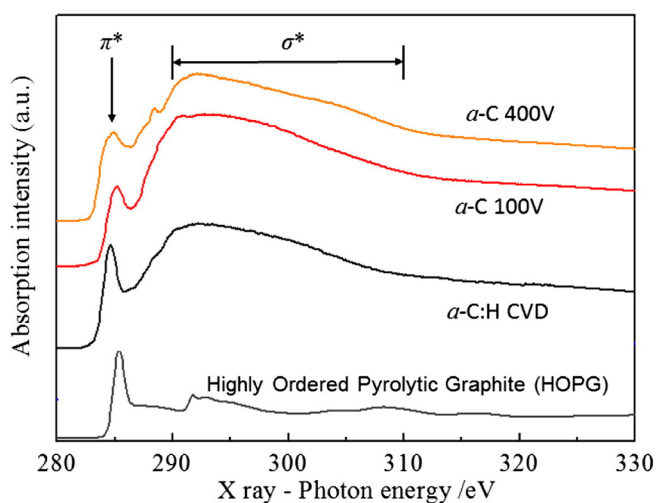


Fig. 3. NEXAFS spectra for *a*-C and *a*-C:H films.

test, film thickness was about 200 nm. Surface images before and after the test were obtained by an atomic force microscope (AFM; SPA300/Seiko Instruments).

To determine the *a*-C:H and *a*-C film structures, all films were also deposited on a silicon (Si) (100) substrate. The thickness of these films was controlled to approximately 100 nm by varying the deposition duration. The elemental composition of each film was determined using Rutherford backscattering (RBS) and elastic recoil detection analysis (ERDA) systems [21]. RBS and ERDA were performed under He⁺ irradiation using an electrostatic accelerator (NT-1700HS; Nisshin-High Voltage Co.). He⁺ ions accelerated to 2.5 MeV were used. The RBS technique was applied to determine the composition of the elements in the sample excluding H. In the ERDA measurement, He⁺ ions collide elastically with H atoms in the sample. The H atoms ejected from the sample were detected with a silicon sensor device (SSD). RBS and ERDA signals were simultaneously detected, and thus the ERDA technique was applied to determine the atomic fraction of H in each sample. Moreover, the *sp*² content in each deposited film was determined by near-edge X-ray absorption fine structure (NEXAFS) spectroscopy. This measurement was performed at the BL09A beam line of New SUBARU at the University of Hyogo. NEXAFS carbon *K*-edge spectra were obtained in the energy range of 275–320 eV with a resolution of 0.5 eV (FWHM) in the total electron yield mode [22,23]. The X-ray beam was irradiated at an angle of 54.7° relative to the normal of the surface of the *a*-C:H film. The monochromator was calibrated relative to the pre-edge resonance at 285.38 eV in the graphite spectrum [24,25].

The SPR measurement system was set up in the Kretschmann configuration [14–16]. The incident light was a beam from a green laser diode with a wavelength of 532 nm. The intensity of the reflected light was measured using a photodetector. The laser diode and photodetector were mounted on separate rotating stages. A flow cell with a volume of approximately 0.21 mL was attached to the top of an SPR device with a multilayer structure to inject the nitric acid onto the *a*-C:H film.

Nitric acid with a concentration of 0.3 mol/L was prepared. The solution was adjusted to this concentration using 60% nitric acid solution

(Kanto Chemical Industries) and deionized pure water. The procedure for investigating the relationship between the *a*-C:H film structure and the chemical resistance was as follows. First, nitric acid solution was injected into a flow cell using a syringe pump and the initial θ_{SPR} was immediately measured. The amount of each solution injected into the cell was controlled using the syringe pump. The injection rate was 2 mL/min. After 15 min, the solution inside the cell was replaced with a new solution and θ_{SPR} was measured again. Subsequently, the solution inside the cell was replaced every 15 min and θ_{SPR} was measured after each replacement.

3. Results

The hydrogen concentration was obtained by RBS/ERDA to investigate the difference between the three films. The two *a*-C films deposited by FCVA exhibited similar RBS/ERDA spectra. Fig. 2 shows the RBS and ERDA spectra for the films deposited by each method. In the RBS spectra, a peak assigned to carbon appeared at 300–400 Ch. In the ERDA spectra, the peak assigned to hydrogen appeared at 300 Ch. The peak for hydrogen for the *a*-C film deposited by FCVA has one-twentieth of the intensity of that for the *a*-C:H film deposited by pulse plasma CVD. From these spectra, the hydrogen content of each film was determined. The hydrogen contents of the two *a*-C films deposited by FCVA were less than 1.5 at.%, which is the lower detection limit for this measurement system. The *a*-C:H films deposited by pulse plasma CVD contained 17 at.% hydrogen, which terminated the bonding network of carbon atoms.

The NEXAFS spectra of the obtained films are shown in Fig. 3. In these spectra, the pre-edge resonance at 285.4 eV is due to the transition from the C1s orbital to the unoccupied π^* orbital, which mainly originates from *sp*² (C=C) sites. The broad band observed at 288–310 eV is assigned to the overlapping C1s to σ^* transitions at the *sp*³, *sp*², and *sp* sites of the *a*-C:H and related films. The absolute *sp*² content was determined by comparison with the spectrum of highly oriented pyrolytic graphite, as shown in Fig. 3 [7]. Table 1 shows the *sp*² content in the *a*-C:H films.

Fig. 4 shows SPR curves for the *a*-C:H film and *a*-C films. Fig. 4a shows the SPR curves for the *a*-C 400 V/Ag multilayer structure over 30 min taken at intervals of 15 min. After 30 min, we could not obtain SPR curves because the *a*-C film had peeled off from the Ag layer. Considering the attenuation of reflected light, the laser incident angle corresponding to the weakest reflectivity was defined as θ_{SPR} . Before the injection of nitrogen solution, the initial θ_{SPR} was 50.34°. The reflectivity at θ_{SPR} rapidly decreased after the injection of nitric acid solution. The SPR angles were 50.34, 50.33, and 50.31° for etching durations of 0, 15, and 30 min, respectively. The shift in θ_{SPR} indicated a decrease in the dielectric constant above the Ag layer surface caused by the decrease in the thickness of the *a*-C film.

To understand microstructural change, although film surface images before and after 1 h immersion tests were obtained, we could not observe the difference. Hence, HNO₃ concentration and etching duration were increased to 2.0 M and 12 h, respectively. Fig. 5 shows AFM images before and after immersion tests. A ten-point average surface roughness, *R*_z, of the surface of the *a*-C 400 V film is changed from 2.6 nm to 3.5 nm by the immersion test of 12 h. On *a*-C 100 V, *R*_z was increased from 0.9 nm to 4.6 nm. Initial value of *R*_z of 2.1 nm was increased to 3.3 nm on *a*-C:H CVD film. Every surface roughness was increased after immersion tests. The surface roughness after 12 h was not a

Table 1
Hydrogen content and *sp*²(*sp*² + *sp*³) ratio in the *a*-C:H and *a*-C films.

Sample name	Hydrogen content (obtained by RBS/ERDA) at.%	<i>sp</i> ² / (<i>sp</i> ² + <i>sp</i> ³) (obtained by NEXAFS) %
<i>a</i> -C 400 V	<1.5	74.3
<i>a</i> -C 100 V	<1.5	54.5
<i>a</i> -C:H CVD	17.0	66.9

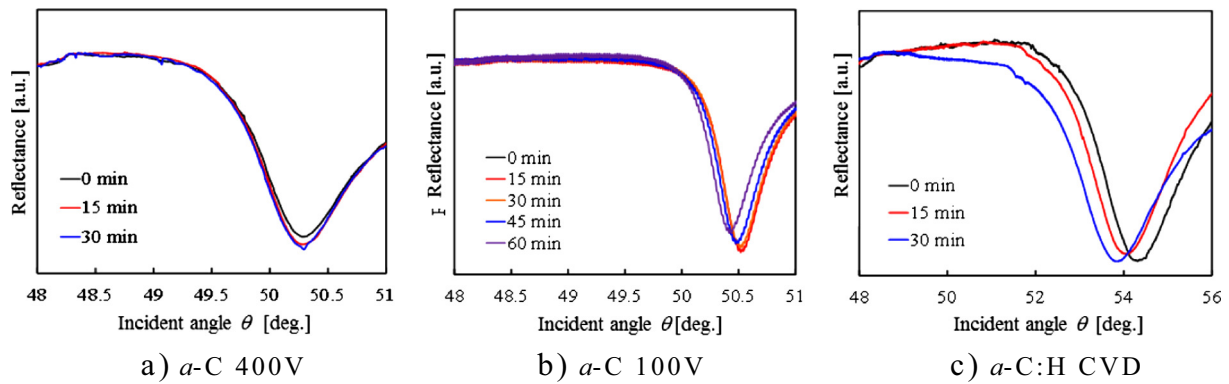


Fig. 4. Reflectivity as a function of laser incident angle in chemical reaction test for 0.3 mol/L nitric acid solution.

uniform roughness because of large island existence. Hence, the meaning of roughness value of R_a or R_z is not matched with actual conditions. Furthermore, the thickness change could not be obtained from these images. These non-uniform areas were smaller than $5 \mu\text{m}$ which is a laser diameter in the SPR measurement. Hence, the obtained SPR data are the average of thickness change on these areas.

To determine the film thickness, the obtained curves were fitted using simulation software based on Fresnel equations (WINSPALL developed by Dr. W. Knoll, MPIP, Germany). This simulation can only be applied to isotropic changes in the film thickness. According to the

simulation, the thickness of the *a*-C 400 V film changed from an initial value of 8.9 nm to 7.7 nm after 30 min. Fig. 4b shows the SPR curves for the *a*-C 100 V/Ag multilayer structure over 60 min taken at intervals of 15 min. SPR curves could not be obtained after 60 min because of peeling at the *a*-C and Ag interface. The initial θ_{SPR} was 50.51° . The SPR angles were $50.51, 50.50, 50.49, 50.48,$ and 50.45° for etching durations of 0, 15, 30, 45, and 60 min, respectively. The film thicknesses were calculated by simulation. The thickness of the *a*-C 100 V film decreased from 6.4 to 5.5 nm after 60 min. Fig. 4c shows the SPR curves for the *a*-C:H CVD/Ag multilayer structure over 30 min at intervals of 15 min. After

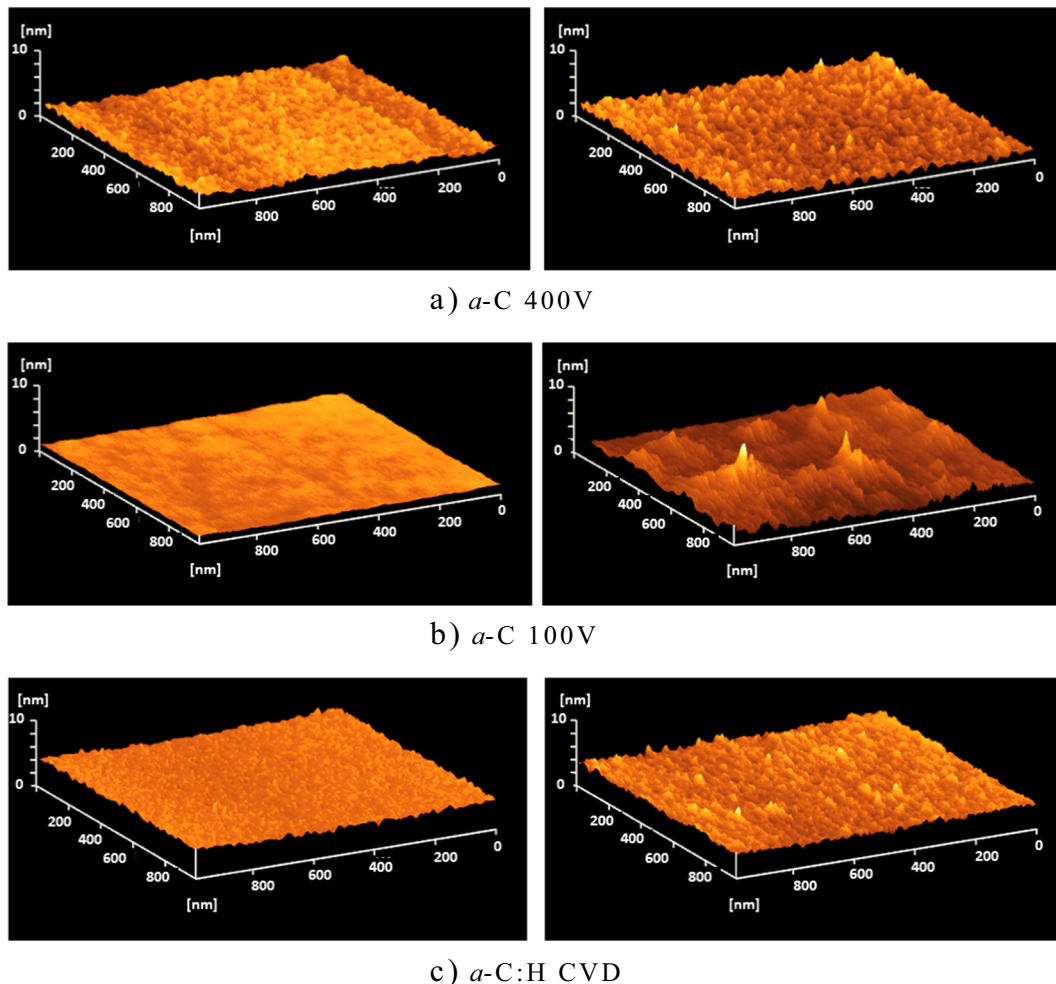


Fig. 5. AFM images before (left) and after (right) the immersion test of 12 h.

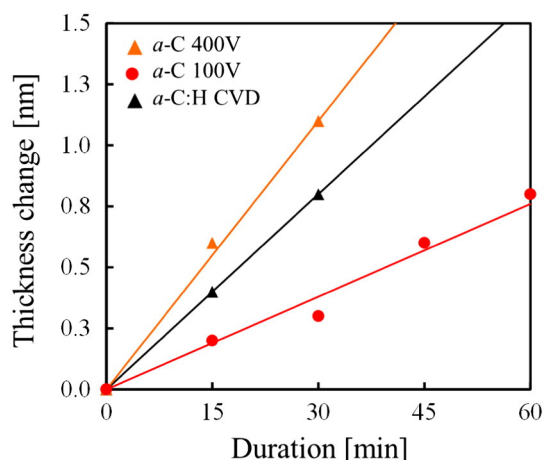


Fig. 6. Change in thickness due to chemical reaction with nitric acid calculated from changes in SPR angle.

30 min, this film also peeled off from the Ag layer. The initial θ_{SPR} was 54.27° , and the SPR angles were 54.27° , 54.02° , and 53.81° for etching durations of 0, 15, and 30 min, respectively. From these data and the simulation, the a-C:H CVD film thickness decreased from 15.5 to 14.7 nm after 30 min. Sasaki et al. reported that the thickness of etched films that can be determined by this SPR method is less than 2 nm [10]. In this study, the film surface was flat in the case of etching by up to 2 nm because the etching was in one direction, whereas the film surface was rough when the amount of etching exceeded 2 nm because the etching started to occur in multiple directions. According to the consideration in this paper, almost any change in the thickness can be detected because the changes obtained were over 2 nm.

Fig. 6 shows the relationship between the change in film thickness and the etching duration derived from the changes in thickness obtained by SPR measurements and the simulations. From Fig. 6, the rate of change in the thickness due to the chemical reaction was determined for the a-C:H and a-C films. The rates of decrease in the film thickness were 2.2, 0.8, and 1.6 nm/h for the a-C 400 V, a-C 100 V, and a-C:H CVD films, respectively. Although 10 time or more certain SPR curves were obtained, SPR curves sometimes were limited to a few curves by the problem of peeling off at interface between carbon film and Ag layer. Hence, SPR data for longest duration of etching evaluation by SPR method was presented in this paper. The trend of all etching rates

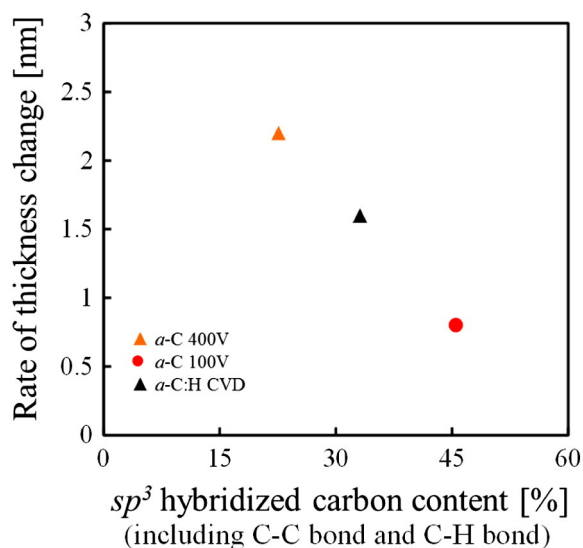


Fig. 7. Relationship between the rate of change in film thickness and sp^3 content in a-C:H and a-C films obtained from NEXAFS spectra.

was similar as the described rates. For all reliable data the order higher rate of change in the thickness was a-C 400 V, a-C:H CVD, a-C 100 V. Hence, trend was not changed. From the ERDA/RBS measurements, the hydrogen contents of the a-C 400 V and a-C 100 V films were both 1.5 at.%, which was the lower detection limit. Although these films had the same hydrogen content, the rates of decrease in the film thickness were markedly different. Furthermore, the rate of change for the a-C:H film with a hydrogen content of 17 at.% was between the rates of change for the two non-hydrogenated films. Hence, the hydrogen content has little effect on the chemical resistance to nitric acid solution. To determine the sp^2/sp^3 ratio dependence, the relationship between the rate of change in the film thickness and the sp^2/sp^3 ratio is shown in Fig. 7. The rate decreased with increasing sp^3 content. Hence, the sp^2/sp^3 ratio has a strong effect on the chemical resistance to nitric acid solution. It is well known that graphite can be etched by nitric acid solution [25,26]. Since the sp^2 components in these a-C:H films are graphite-like components, these results suggest that the sp^2 components in the a-C:H films selectively react with nitric acid solution. In the case of nitric acid, the sp^2 content is an important structural factor determining the chemical resistance.

4. Conclusion

Changes in the thickness of a-C:H films and the rate of change upon their reaction with nitric acid were determined using an SPR device with an a-C:H/Ag/glass multilayer structure. To investigate the structural dependence of the corrosion resistance of a-C:H films, three types of film with different structures were deposited on a metal surface to estimate the change in the film thickness due to the chemical reaction using the SPR phenomenon. Two non-hydrogenated a-C films and one hydrogenated a-C:H film were synthesized to estimate the effects of the sp^2/sp^3 ratio and hydrogenation, respectively. The rates of decrease in the thickness were 2.2, 0.8, and 1.6 nm/h for the a-C films with the lower and higher sp^2 contents and the 17 at.% hydrogenated a-C:H film, respectively. Although the hydrogen content did not affect the rate of change in the film thickness, the rate of change clearly decreased with decreasing sp^2/sp^3 ratio. These results indicate that the sp^2/sp^3 ratio is an important factor determining the chemical resistance to nitric acid solution.

Prime novelty statement

To investigate the structural dependence of the corrosion resistance of amorphous carbon films against nitric acid solution, etching of different types of amorphous carbon films by nitric acid was evaluated using surface plasmon resonance device with a multilayer structure consisting of an amorphous carbon layer on Ag. The rate of change in film thickness affected the hydrogen content a little and clearly decreased with decreasing sp^2/sp^3 ratio, and these results indicate that the sp^2/sp^3 ratio is an important factor determining the chemical resistance to nitric acid solution.

Acknowledgments

We would like to thank for iMott Inc. for the FCVA deposition. This work was supported by the Tokyo Tech Engineering Grant for New Associate Professor, and the MIKIYA Science and Technology Foundation.

References

- [1] M. Hiratsuka, H. Nakamori, Y. Kogo, M. Sakurai, N. Ohtake, H. Saitoh, Correlation between optical properties and hardness of diamond-like carbon films, *J. Solid Mech. Mater. Eng., Jpn. Soc. Mech. Eng.* 7 (2013) 187–198.
- [2] N. Ohtake, Mechanical properties of silicon-doped diamond-like carbon films prepared by pulse-plasma chemical vapor deposition reference, *Surf. Coat. Technol.* 206 (2011) 1011–1015.

- [3] E.L. Dalibon, R. Charadia, A. Cabo, V. Trava-Airoldi, S.P. Brühl, Evaluation of the mechanical behaviour of a DLC film on plasma nitrided AISI 420 with different surface finishing, *Surf. Coat. Technol.* 235 (2013) 735–740.
- [4] J. Robertson, Diamond-like amorphous carbon, *Mater. Sci. Eng. R* 37 (2002) 129–281.
- [5] A. Grill, Diamond-like carbon: state of the art, *Diam. Relat. Mater.* 8 (1999) 428–434.
- [6] J. Robertson, Deposition mechanism of a-C and a-C:H, *J. Non-Cryst. Solids* 164–166 (1993) 1115–1118.
- [7] J. Lee, R.W. Collins, V.S. Veerasamy, J. Robertson, Analysis of the ellipsometric spectra of amorphous carbon thin evaluation of the sp^2 -bonded carbon content, *Diam. Relat. Mater.* 7 (1998) 999–1009.
- [8] M. Ban, T. Yuhara, Chemical resistance of DLC thin film deposited PMMA substrates, *Surf. Coat. Technol.* 203 (2009) 2587–2590.
- [9] K. Kurihara, K. Nakamura, K. Suzuki, Asymmetric SPR sensor response curve-fitting equation for the accurate determination of SPR resonance angle, *Sensors Actuators B* 86 (2002) 49–57.
- [10] Yasushi Sasaki, Aoi Takeda, Kiyoto Ii, Shigeo Ohshio, Hiroki Akasaka, Masayuki Nakano, Hidetoshi Saitoh, Evaluation of etching on amorphous carbon films in nitric acid, *Diam. Relat. Mater.* 24 (Jan. 2012) 104–106.
- [11] B. Liedberg, C. Nylander, I. Lundstrom, Biosensing with surface plasmon resonance—how it all started, *Biosens. Bioelectron.* 10 (1995) 1–9.
- [12] R.W. Wood, On a remarkable case of uneven distribution of light in a diffraction grating spectrum, *Philos. Mag.* 4 (8) (1902) 396–402.
- [13] R.W. Wood, Diffraction gratings with controlled groove form and abnormal distribution of intensity, *Philos. Mag.* 23 (1912) 310–317.
- [14] L. Rayleigh, Dynamical theory of the grating, *Proc. R. Soc. A London* 79 (1907) 399.
- [15] U. Fano, The theory of anomalous diffraction gratings and of quasi-stationary waves on metallic surfaces, *J. Opt. Soc. Am.* 31 (1941) 213–222.
- [16] E. Kretschmann, Die Bestimmung optischer Konstanten von Metallen durch Anregung von Oberflächenplasmaschwingungen, *Z. Phys.* 241 (1971) 313–324.
- [17] S. Kishimoto, S. Ohshio, H. Akasaka, H. Saitoh, Detection of protein adsorption on silica surface using surface plasmon resonance sensor, *Jpn. J. Appl. Phys.* 47 (2008) 8106–8108.
- [18] H. Akasaka, N. Gawazawa, S. Kishimoto, S. Ohshio, H. Saitoh, Surface plasmon resonance detection using amorphous carbon/Au multilayer structure, *Appl. Surf. Sci.* 256 (2009) 1236–1239.
- [19] V.S. Veerasamy, G.A.J. Amaratunga, W.I. Milne, J. Robertson, P.J. Fallon, Influence of carbon ion energy on properties of highly tetrahedral diamond-like carbon, *J. Non-Cryst. Solids* 164–166 (1993) 1111–1114.
- [20] S. Fujimoto, N. Ohtake, O. Takai, Mechanical properties of silicon-doped diamond-like carbon films prepared by pulse-plasma chemical vapor deposition, *Surf. Coat. Technol.* 206 (2011) 1011–1015.
- [21] Y. Ohkawara, S. Ohshio, T. Suzuki, H. Ito, K. Yatsui, H. Saitoh, Dehydrogenation of nitrogen-containing carbon films by high-energy He^{2+} irradiation, *Jpn. J. Appl. Phys.* 40 (2001) 3359–3363.
- [22] K. Kanda, Y. Shimizugawa, Y. Haruyama, I. Yamada, S. Matsui, T. Kitagawa, H. Tsubakino, T. Gejo, NEXAFS study on substrate temperature dependence of DLC films formed by Ar cluster ion beam assisted deposition, *Nucl. Instrum. Methods Phys. Res., B* 206 (2003) 880–883.
- [23] A. Saikubo, N. Yamada, K. Kanda, S. Matsui, T. Suzuki, K. Niihara, H. Saitoh, Comprehensive classification of DLC films formed by various methods using NEXAFS measurement, *Diam. Relat. Mater.* 17 (2008) 1743–1745.
- [24] P.E. Batson, Carbon 1s near-edge-absorption fine structure in graphite, *Phys. Rev. B* 48 (1993) 2608–2610.
- [25] Y.-R. Shin, S.-M. Jung, I.-Y. Jeon, J.-B. Baek, The oxidation mechanism of highly ordered pyrolytic graphite in a nitric acid/sulfuric acid mixture, *Carbon* 52 (2013) 493–498.
- [26] E. Bouleghimat, P.R. Davies, R.J. Davies, R. Howarth, J. Kulhavy, D.J. Morgan, The effect of acid treatment on the surface chemistry and topography of graphite, *Carbon* 61 (2013) 124–133.